Korean J. Chem. Eng., 40(1), 248-254 (2023)
DOI: 10.1007/s11814-022-1212-2

pISSN: 0256-1115
eISSN: 1975-7220

Minimum elutriation velocity of the binary solid mixture - Empirical correlation and genetic algorithm (GA) modeling

Sudipta Let*, Nirjhar Bar*,, Ranjan Kumar Basu*, and Sudip Kumar Das*,†**

*Department of Chemical Engineering, University of Calcutta, 92, A. P. C. Road, Kolkata - 700 009, India
**Present address: St. James' School, 165, A. J. C. Bose Road, Kolkata - 700 014, West Bengal, India
(*Received 20 April 2022 • Revised 14 June 2022 • Accepted 19 June 2022*)

Abstract−The solid-water fluidized bed was investigated with a binary mixture of irregularly shaped sand particles. A binary mixture was produced by mixing particles of sand for different weight ratios. The influence of various operating parameters on minimum elutriation velocity was investigated. It was observed that the U_{me} decreases with the increase of the lighter particles in the binary mixture, and the U_{me} increases with the increase of column diameter. A simplified empirical correlation has been developed to predict minimum elutriation velocity with acceptable statistical parameters. Application concerning a hybrid of artificial neural network (ANN), and genetic algorithm (GA), is successfully predicted.

Keywords: Minimum Elutriation Velocity, Solid-liquid Fluidized Bed, GA-ANN

INTRODUCTION

In the fluidized condition, solid particles are in the freeboard area. They can be removed from the bed on increasing fluid velocity further by a process called elutriation. For mixed-sized particles of constant density, elutriation occurs when smaller particles are continuously removed by fluid velocity from a bed of wide particle size. It is an actual practical problem in the fluidized bed operation, mainly if the freeboard height is low. The axial solid distribution differs considerably for the fluidized beds' low and high freeboard heights of the fluidized beds [1]. Minimum elutriation velocity U_{me} is the maximum fluid velocity of a solid particle carried out from the bed. The literature review suggested that much work has been reported on elutriation for gas-solid fluidized system [2-6]. Many correlations have been proposed to predict the elutriation rate constant [7-9]. However, the same for liquid-solid fluidized beds is limited, especially for binary solid particle mixtures.

Misra et al. [10] studied the influence of surface tension of a liquid on elutriation in a cylindrical column's coal-water (solid-liquid) system. Maiti et al. [11] reported elutriation characterization for solid-liquid (non-Newtonian) fluidized systems and developed an empirical correlation. Ganguly [12] estimated the elutriation velocity for a binary mixture of solids varying in size and density in the solid-water fluidized system. Ganguly [13] studied the effect of different parameters on the equilibrium mass fraction of the elutriating component in the bed and proposed a correlation to predict it. A modified correlation incorporating sphericity of solid was developed by Ganguly [14]. Stojkovski and Kostic [15] and Ma et al. [16] summarized published empirical correlations based on the elutriation rate constant.

One of the most advanced computational techniques is the hybrid computational technique of amalgamating GA and Levenberg-Marquardt (LM) algorithm to predict unknown data. The genetic algorithm (GA) application has increased exponentially in the last two decades [17-24]. The use of ANN to predict U_{me} has been reported by Maiti et al. [11]. However, the prediction of minimum elutriation velocity using GA was not reported in the past.

The fundamental quantitative description of entrainment and elutriation for the gas-solid fluidized system was described by Miyahara et al. [1,6,25]. The literature review suggests that only a few articles are available for liquid-solid fluidized systems [11]. Hence, this study is intended to generate experimental data on the elutriation of the solid-liquid fluidized system using irregular-shaped binary sand particles. The variation of the operating parameters on elutriation has been thoroughly discussed.

An empirical equation was developed to estimate the minimum elutriation velocity U_{me} with all measurable operating variables. The applicability of the hybrid GA-ANN was tested. Existing correlations were re-evaluated. Elutriation velocity was found to be a function of particle terminal settling velocity; hence the ratio of U_{me}/U_t is used to develop the empirical correlation.

EXPERIMENTAL

The experimental setup included transparent Perspex fluidizing columns with diameters of 0.072 m and 0.054 m, with 1.3 m and 1.5 m in height, respectively. The experimental setup consists of a test section, liquid storage tank (0.45 m^3), centrifugal pump (2 HP motor, Motor Crompton, India), rotameter (Transducer and Controls Pvt. Ltd., Hyderabad, India, accuracy ±2%), manometer and control valves, shown in Fig. 1(a) and photograph in Fig. 1(b). A 16-mesh stainless steel screen was fitted to separate the bed particles at the bottom section. It is followed by a conical brass calming section, in-between space of stainless-steel mesh and a conical section filled with glass beads of different sizes to ensure the homogeneous flow

†To whom correspondence should be addressed.
E-mail: drsudipkdas@gmail.com, skdchemengg@caluniv.ac.in

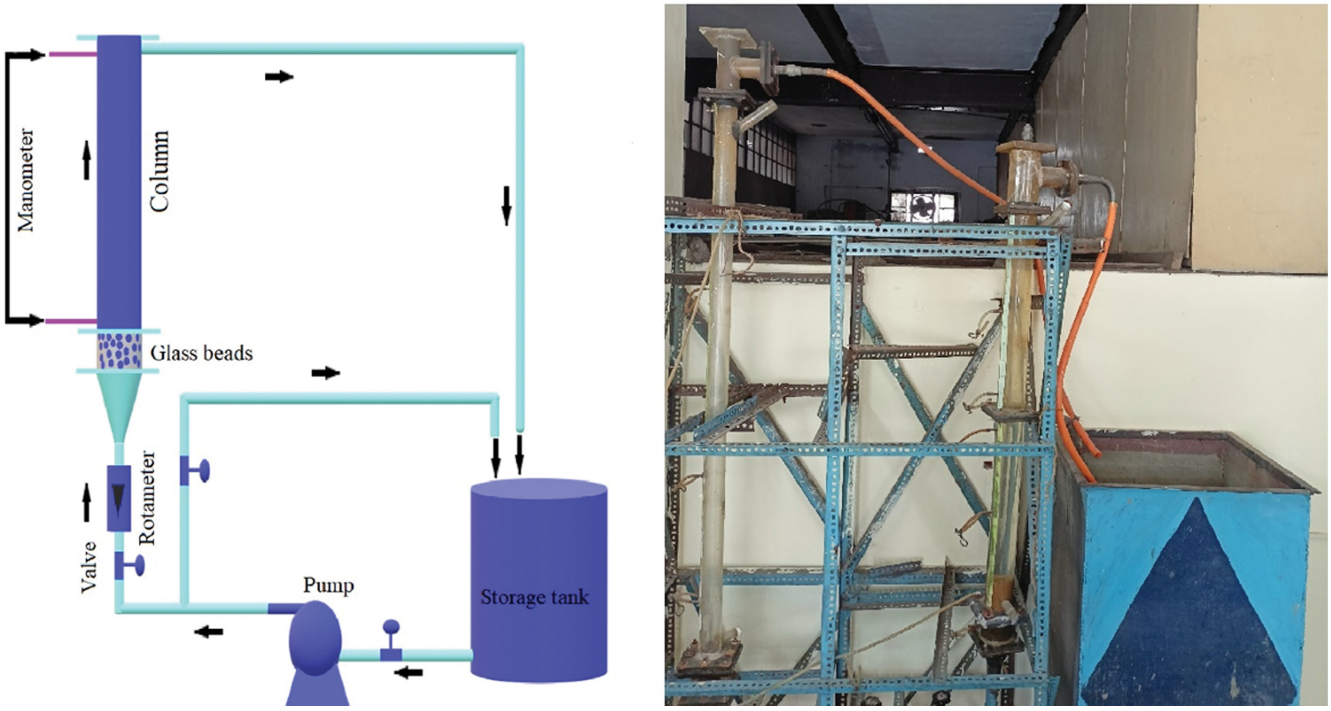

Fig. 1. Schematic diagram of the experimental setup.

Table 1. Range of experimental data

Measurement type	Range	
Input parameters	Average particle diameter, d_M, m	0.000324-0.00071
	Column diameter, d_t, m	0.054-0.072
	Sphericity, Φ_M, dimensionless	0.7113-0.8833
	Initial bed height, H_o, m	0.15-0.288
Output parameters	Minimum elutriation velocity, U_{me}, m/s	0.029247-0.172628

of fluid through the column. The detailed dimensions of the column are reported in our earlier paper [16]. Water was pumped from the storage tank to introduce it into the column for the elutriation of a binary mixture of sand at 1 m height. The temperature was maintained at 28 °C±2 °C by circulating tap water through a copper coil into the storage tank. Each set of increases in water velocity pressure drop across the bed was recorded with an inclined manometer (Mercury beneath water type arrangement). A rotameter measures the liquid flow rate and collects the liquid at the discharge point in a specific time interval. The experimental setup and procedure have been elaborated in the previous publication [17,24].

The physical properties of the solid particle and detailed computation procedure of mean particle diameter d_M and mean sphericity ϕ_M for each set of a binary mixture of solids varying in size are mentioned in our previous publication [17]. The range of variables investigated is shown in Table 1.

RESULTS AND DISCUSSION

1. Determination of Minimum Elutriation Velocity

For a binary mixture, various degrees of heterogenicity were cre-

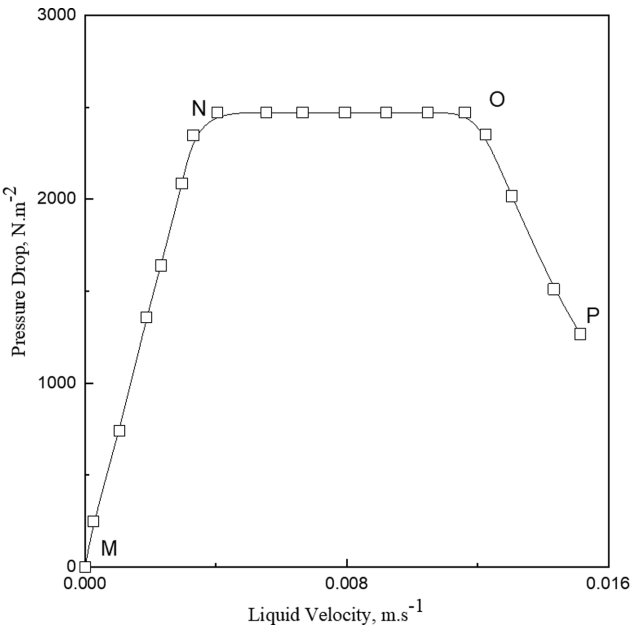

Fig. 2. Bed pressure drop vs liquid velocity.

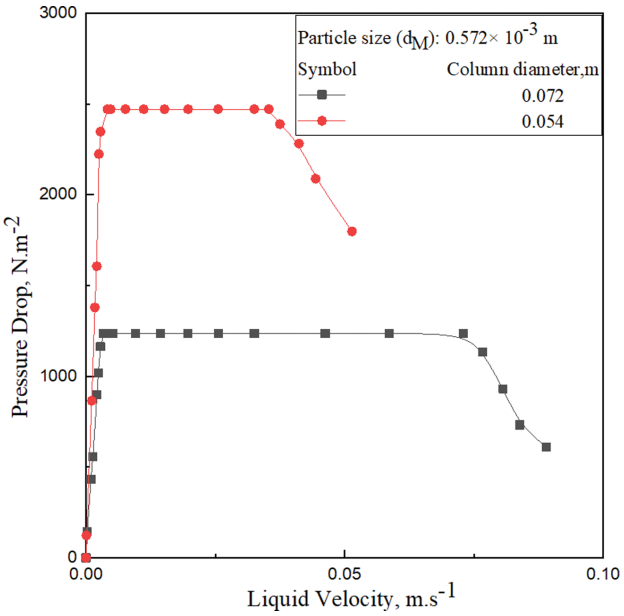

Fig. 3. Distinctive elutriation plot for constant bed weight.

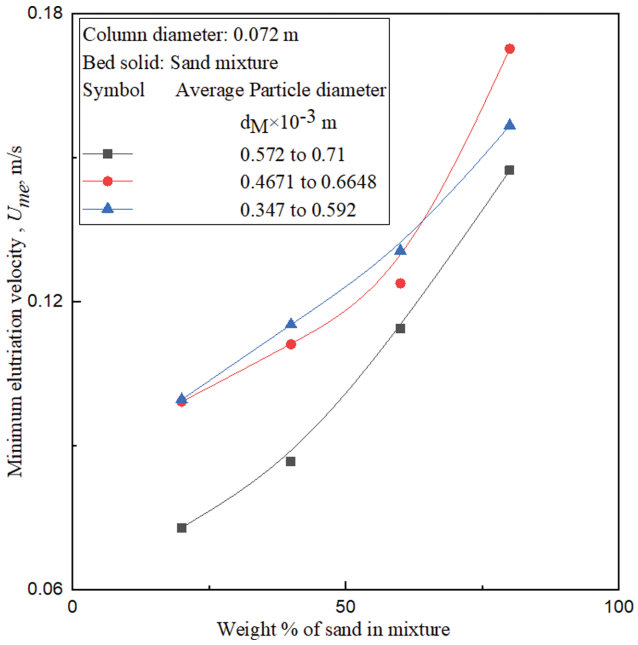

Fig. 4. Variation of U_{me} for different % of binary mixture of particles.

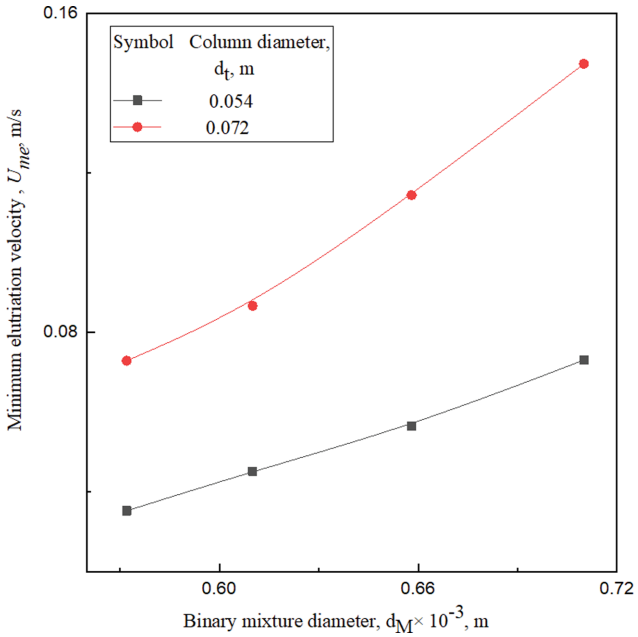

Fig. 5. Variation of U_{me} at different column diameter.

ated in the mixture by varying the weight ratio of each component. Water was introduced into the column at an increasing rate, and the corresponding pressure drop across the column for an individual set of the binary mixture was recorded. The pressure drops across corresponding liquid velocity, the minimum elutriation velocity, U_{me} were evaluated graphically, Fig. 2. The pressure difference existing across the bed with increasing liquid velocity was plotted. The corresponding velocity of the point at which N-O and O-P intersect represents minimum elutriation velocity, U_{me}. Fig. 3 depicts distinctive elutriation curves. Pressure difference remains constant after fluidization up to a definite liquid velocity, i.e., U_{me}, beyond which the pressure difference decreases sharply, almost linearly.

2. Influence of Various Operating Parameters

Freeboard height is an essential parameter for the elutriation process, defined as the height of a column that is not occupied by solid particles. When bed weight is constant, static bed height decreases with an increase in column diameter, consequently increasing the freeboard height and requiring increased liquid flow to elutriate particles. At constant bed weight, the minimum elutriation velocity, U_{me}, increases with the increase in column diameter, Fig. 3. The increased column diameter for the constant bed weight increases the freeboard height [13,26].

The minimum elutriation velocity increases with the mean particle sizes of binary mixture for constant bed weight in column diameter, as shown in Figs. 4 and 5. Geldart et al. [27] have already reported a similar result for a gas-solid system. The minimum fluidization and elutriation velocity increase with the proportion of coarse particles [28]. With the increase in mean particle diameter of a binary mixture, more buoyant and drag force is required to elutriate that mixture, i.e., increases in the liquid velocity.

3. Correlation

In a binary mixture of sand particles, the elutriation mechanism involves transferring particles of smaller diameter from the particles of larger diameter. The smaller diameter particles enter the freeboard space first and then carry out from the column. Most researchers proposed a correlation involving elutriation using rate constants and dimensionless form [7,29,30]. In the dimensionless form, most of them introduced terminal settling velocity. Hence, in the present case, the ratio of the minimum elutriation velocity to the terminal settling velocity is a function of the operating variables, in the dimensionless form as,

$$\frac{U_{me}}{U_t} = \left(\frac{d_t}{d_M}, \frac{H_f}{H_O}, \phi_M\right) \quad (1)$$

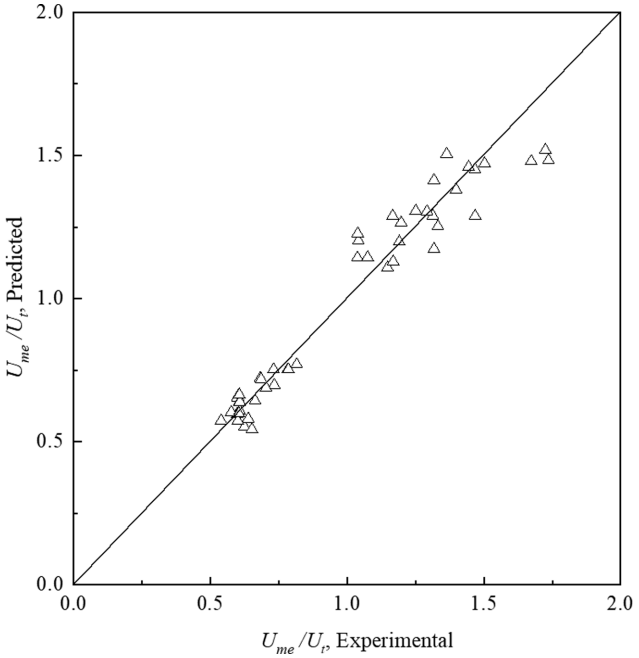

Fig. 6. Comparison between experimental and calculated U_{me}/U_t from Eq. (2).

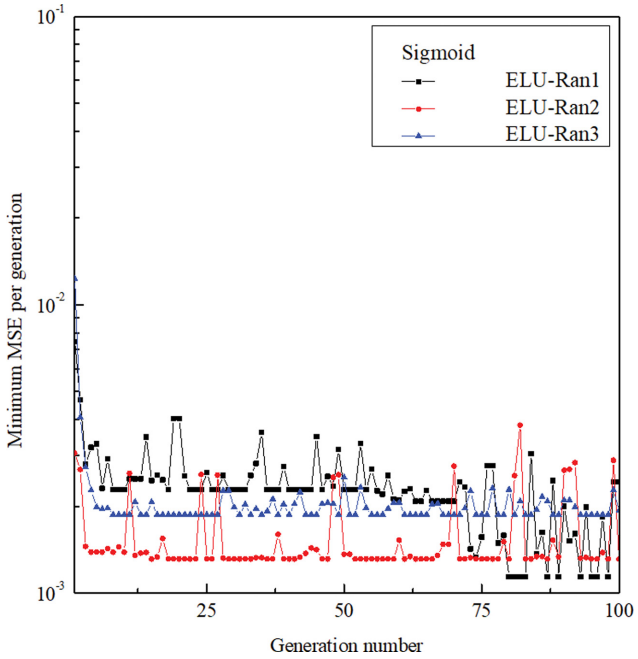

Fig. 7. Variation of minimum value of cross-validation with respect to number of processing elements in hidden layer for sigmoid transfer function.

The multiple linear regression (MLR) analysis deduced the following equation to predict the ratio binary mixture of irregularly shaped sand particles in water,

$$\left(\frac{U_{me}}{U_t}\right)=28.981\times\left(\frac{d_t}{d_m}\right)^{-1.121\pm0.188}\times\left(\frac{H_f}{H_O}\right)^{1.712\pm0.098}\times\phi_M^{3.048\pm0.068} \quad (2)$$

with the following range of variables,

$$0.5389\le\frac{U_{me}}{U_t}\le1.7361$$

$$76.05\le\frac{d_t}{d_M}\le222.35$$

$$3.4722\le\frac{H_f}{H_o}\le6.6667$$

$$0.7113\le\phi_M\le0.8833$$

Eq. (2) consists of the following statistical parameters: correlation coefficient, 0.9699; SD, 0.0461; RE, 0.0649; AE, 0.0052 and MSE,: 0.0003 for a *t*-value of 2.0137 with 44 degrees of freedom. The correlation plot is presented in Fig. 6.

4. GA Analysis

Particle diameter, d_M, column diameter, d_t, Initial bed height, H_o, and sphericity, ϕ_M represent the parameters used for input, while U_{me} the output is to be predicted. The range related to these parameters can be observed in Table 1. The first important task for machine learning and statistical/mathematical data analysis was to remove any error related to randomness from the data used for analysis. Therefore, the experimental data was first divided into three different spread sheet files: ELU-Ran$_1$, ELU-Ran$_2$, and ELU-Ran$_3$. The randomization process was done separately to eliminate errors related to randomization.

After this stage, the data of each file were divided into three divi-

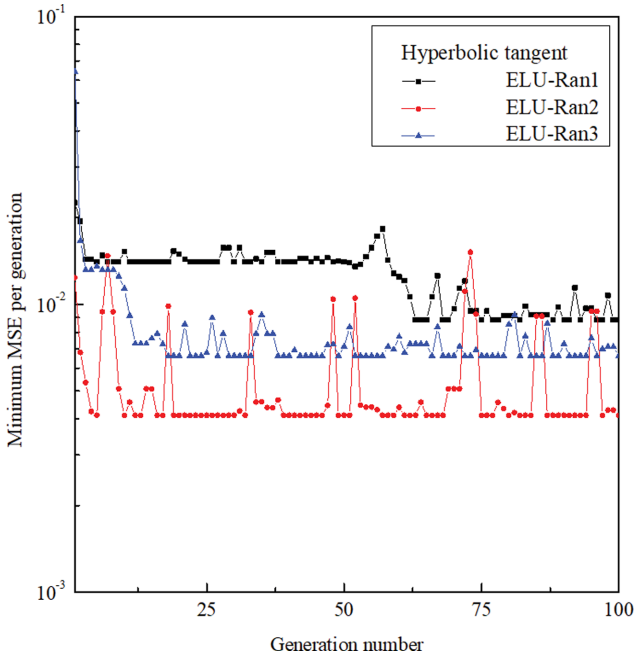

Fig. 8. Variation of minimum value of cross-validation with respect to number of processing elements in hidden layer for hyperbolic tangent transfer function.

sions having 10% (for unknown data prediction), 20% (for cross-validation) and 70% (for training), respectively. The mutation probability value (0.1) and probability value for the crossover operator (0.9) were fixed for this analysis. The network structure varied from 1 to 10 processing elements (during the application associated

Table 2. Performance of the optimized hybrid network for minimum elutriation velocity U_{me}

Transfer function	Randomization No.	Minimum average fitness	RE	AE	SD (σ)	MSE	CCC (R)	χ^2
Sigmoid	**ELU-Ran1**	**0.00114**	**0.118681**	**0.010104**	**0.076052**	**0.000166**	**0.946181**	**0.01023**
	ELU-Ran2	0.001311	0.204289	0.017354	0.15238	0.000427	0.774188	0.020382
	ELU-Ran3	0.001871	0.178866	0.010414	0.20971	0.00017	0.899092	0.011333
Hyperbolic tangent	ELU-Ran1	0.00881	0.216827	0.018751	0.099585	0.000475	0.930813	0.033772
	ELU-Ran2	0.00411	0.133561	0.011705	0.120682	0.000222	0.961996	0.010388
	ELU-Ran3	0.006627	0.193934	0.014755	0.108645	0.000267	0.837319	0.020417

with LM algorithm). Here, the population number of 6 was used to find the optimal structure of network configuration. The transfer function *tanh* (hyperbolic tangent) and the sigmoid type algorithms were attempted separately.

Figs. 7 and 8 present the optimized processes graphically to determine the optimal generation. The minimum generation error for the analysis is ~10^{-3} (2^{nd} column of Table 2). They represent the variation and its subsequent determination concerning the least value of error associated with a particular generation number when these two transfer functions are used. Once the network structures are fully optimized, the 10% unknown data prediction (kept separately for the output prediction) related to ELU-Ran_1, ELU-Ran_2, and ELU-Ran_3, respectively, is used. Table 2 gives the result of the output prediction. The careful observation of Table 2, (Figs. 9 and 10) shows that the last prediction of this GA is successful.

5. Comparison with Existing Results (from Literature Review)

The experimental results were compared with existing correlations and shown in Table 3. The comparison was performed with the help of the error parameters mentioned below:

$$\text{Absolute error, } AE = \frac{1}{N}\sum\left|(U_{me})_{exp} - (U_{me})_{cal}\right| \quad (5)$$

$$\text{Relative error, } RE = \frac{1}{N}\sum\left|\frac{(U_{me})_{exp} - (U_{me})_{cal}}{(U_{me})_{exp}}\right| \quad (6)$$

Table 3 indicates that the AE (average relative error) as well as RE (average absolute error) for present Eq. (2) is less than the other published correlation. The first equation in Table 3, i.e., Eq. (3) proposed by Ganguly [12], does not include the sphericity term, although particles are irregularly shaped. In Eq. (4), Ganguly [14] included the sphericity term, but the equation does not give a satisfactory result. Only sand particles are used as solid and water in the fluidized bed in the present case.

The present research involves computation using GA-ANN type to analyze and predict minimum elutriation velocity in a fluidized bed and compare these results with different correlations that are in existence. Here, this GA-ANN prediction is found to be comparable to other processes. It is beneficial for predicting other parameters connected with the fluidized bed.

CONCLUSION

The elutriation of a binary mixture of irregularly shaped particles in water was experimentally investigated for the influence of vari-

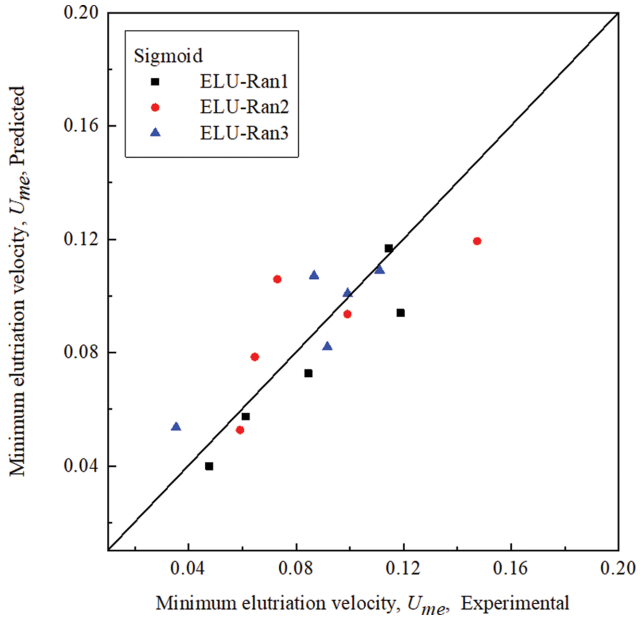

Fig. 9. Comparison between experimental and predicted U_{me}.

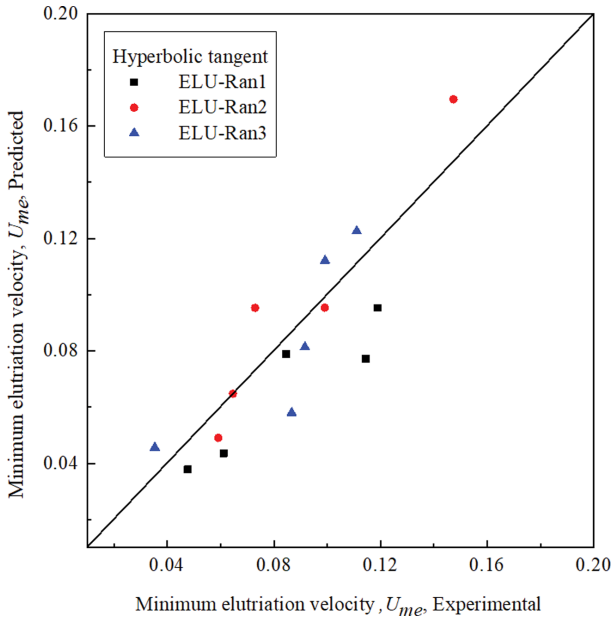

Fig. 10. Comparison between experimental and predicted U_{me}.

Table 3. Proposed correlation in literature for the prediction of minimum elutriation velocity, AE and RE have been calculated on the basis of U_{me}

Sl. No.	Reference	Equations		Range of parameters	RE, %	AE, %
1	[12]	$Re_{me}=2.75\times10^{4}\left(\frac{d_p}{d_t}\right)^{1.71}\left[\frac{(\rho_s-\rho_l)}{\rho_l}\right]^{0.47}\left(\frac{H}{H_s}\right)^{0.19}$	(3)	$0.67\le\frac{(\rho_s-\rho_l)}{\rho_l}\le3.33$ $0.0039\le\left(\frac{d_p}{d_t}\right)\le0.0096$ $2.74\le\left(\frac{H}{H_s}\right)\le23.21$	66.96	5.74
2	[14]	$\frac{U_{me}}{U_{mf}}=115.71(Ar)^{-0.274}\left(\frac{H}{H_s}\right)^{0.204}(\phi_s)^{0.568}$	(4)	$90\le Ar\le48342$ $2.78\le\frac{H}{H_s}\le23.70$ $0.363\le\phi_s\le0.975$	38.78	3.66
3	Present study	$\left(\frac{U_{me}}{U_t}\right)=28.981\times\left(\frac{d_t}{d_m}\right)^{-1.121}\times\left(\frac{H_f}{H_O}\right)^{1.712}\times\phi_M^{3.048}$	(2)	$0.5389\le\frac{U_{me}}{U_t}\le1.7361$ $76.05\le\frac{d_t}{d_M}\le222.35$ $3.4722\le\frac{H_f}{H_o}\le6.6667$ $0.7113\le\phi_M\le0.8833$ $693.75\le Ar\le7313.88$	6.49	0.52
4	GA-ANN study				11.86	1.01

ous physical and dynamic variables on elutriation. The minimum elutriation velocity decreased to the mixture's increasing lighter particle weight ratio. The higher the column diameter, the higher the minimum elutriation velocity. The empirical correlation that has been proposed for elutriation for binary mixture is statistically acceptable. The applicability of the GA-ANN modeling to predict the minimum elutriation is described. The effects of particle density will be studied in the future.

ACKNOWLEDGEMENT

SL is grateful to the University Grants Commission (UGC), India, for his fellowship under grant F1-17.1/2017-18/RGNF-2017-18-SC-WES-40957/(SA-III/Website) dated 13.07.2017.

NOMENCLATURE

Symbols

d : diameter [m]
g : gravitational force [m/s^2]
H_o, H_s : initial bed height [m]
H_f, H : free-board height [m]
U_{me} : minimum elutriation velocity [m/s]
U_{mf} : minimum fluidization velocity [m/s]
U_t : free fall terminal settling velocity [m/s]

AE : relative absolute error, $AE=\frac{1}{N}\sum\left|(U_{me})_{exp}-(U_{me})_{cal}\right|$

Ar : Archimedes number, $\frac{g d_M^3\rho_l(\rho_M-\rho_l)}{\mu_l^2}$, dimensionless

Re : Reynolds number, $\frac{U_l d_M\rho_l}{\mu}$, dimensionless

RE : average Relative error, $RE=\frac{1}{N}\sum\left|\frac{(U_{me})_{exp}-(U_{me})_{cal}}{(U_{me})_{exp}}\right|$

MSE : mean Squared error, $MSE=\frac{1}{N}\sum_{i=1}^{N}(x_i-y_i)^2$, dimensionless

Sigmoid : transfer function, $f_h(x)=\frac{1}{(1+e^{-\beta x})}$, dimensionless

Tangent hyperbolic : transfer function, $f_h(x)=\tanh\beta x=\frac{(e^{\beta x}-e^{-\beta x})}{(e^{\beta x}+e^{-\beta x})}$, dimensionless

Greek Letters

ϕ : sphericity, dimensionless
ρ : density [kg/m^3]
μ : viscosity [N/m^2]
χ^2 : $\chi^2=\sum_{i=1}^{N}\frac{(x_i-y_i)^2}{y_i}$, dimensionless
σ : $\sigma=\sqrt{\sum_{i=1}^{N}\frac{1}{(N-1)}\left[\left(\frac{y_i-x_i}{x_i}\right)-AARE\right]^2}$

Subscripts and Superscripts

i : ith fraction
l : liquid
M : mixture
s : solid
t : column

mf : minimum fluidization
cal : calculated
exp : experimental

REFERENCES

1. T. Miyahara, K. Tsuchiya and L.-S. Fan, *AIChE J.*, **35**, 1195 (1989).
2. J.-H. Choi, J.-M. Suh, I.-Y. Chang, D.-W. Shun, C.-K. Yi, J.-E. Son and S.-D. Kim, *Powder Technol.*, **121**, 190 (2001).
3. J. Li, A. Yamashita and K. Kato, *J. Chem. Eng. Jpn.*, **33**, 730 (2000).
4. D. Santana, J. M. Rodríguez and A. Macías-Machín, *Powder Technol.*, **106**, 110 (1999).
5. K. Smolders and J. Baeyens, *Powder Technol.*, **92**, 35 (1997).
6. E. R. Monazam, R. W. Breault, J. Weber and K. Layfield, *Powder Technol.*, **305**, 340 (2017).
7. M. Colakyan and O. Levenspiel, *Powder Technol.*, **38**, 223 (1984).
8. K. Kato, S. Kanbara, T. Tajima, H. Shibasaki, K. Ozawa and T. Takarada, *J. Chem. Eng. Jpn.*, **20**, 498 (1987).
9. J. M. Rodríguez, J. R. Sánchez, A. Alvaro, D. F. Florea and A. M. Estévez, *Powder Technol.*, **111**, 218 (2000).
10. P. Misra, S. K. Sawarkar and U. P. Ganguly, *Int. J. Miner. Process.*, **32**, 311 (1991).
11. S. B. Maiti, N. Bar and S. K. Das, *Adv. Powder Technol.*, **30**, 2940 (2019).
12. U. P. Ganguly, *Can. J. Chem. Eng.*, **60**, 466 (1982).
13. U. P. Ganguly, *Can. J. Chem. Eng.*, **60**, 470 (1982).
14. U. P. Ganguly, *Can. J. Chem. Eng.*, **67**, 162 (1989).
15. V. Stojkovski and Z. Kostić, *Therm. Sci.*, **7**, 43 (2003).
16. X. Ma, Y. Honda, N. Nakagawa and K. Kato, *J. Chem. Eng. Jpn.*, **29**, 330 (1996).
17. S. Let, N. Bar, R. K. Basu and S. K. Das, *Chem. Eng. Technol.*, **45**, 73 (2022).
18. I. Ghosh, S. Kar, T. Chatterjee, N. Bar and S. K. Das, *Sustain. Chem. Pharm.*, **19**, 100374 (2021).
19. K. Ghosh, N. Bar, A. B. Biswas and S. K. Das, *Can. J. Chem. Eng.*, **97**, 2883 (2019).
20. K. Ghosh, N. Bar, A. B. Biswas and S. K. Das, *Sustain. Chem. Pharm.*, **19**, 100370 (2021).
21. S. Nag, N. Bar and S. K. Das, *Chem. Eng. Sci.*, **226**, 115904 (2020).
22. S. Nag, A. Mondal, D. N. Roy, N. Bar and S. K. Das, *Environ. Technol. Innov.*, **11**, 83 (2018).
23. S. Nag, N. Bar and S. K. Das, *Environ. Technol. Innov.*, **13**, 130 (2019).
24. S. Let, N. Bar, R. K. Basu and S. K. Das, *Part. Sci. Technol.*, Online (2022), doi:10.1080/02726351.2022.2056551.
25. C. Y. Wen and L. H. Chen, *AIChE J.*, **28**, 117 (1982).
26. S. K. Guha, A. Kumar and P. S. Gupta, *Can. J. Chem. Eng.*, **50**, 602 (1972).
27. D. Geldart, J. Baeyens, D. J. Pope and P. Van De Wijer, *Powder Technol.*, **30**, 195 (1981).
28. S. B. Maiti, S. Let, N. Bar and S. K. Das, *Chem. Eng. Sci.*, **176**, 233 (2018).
29. M. Colakyan, N. Catipovic, G. Jovanovic and F. Fitzgerald, *AIChE Symp. Ser.*, **77**, 66 (1981).
30. J.-H. Choi, K.-B. Choi, P. Kim, D.-W. Shun and S.-D. Kim, *Powder Technol.*, **92**, 127 (1997).